Geophysical Research Letters

Supporting Information for

On the Cause of Recent Variations in Stratospheric Ozone

Martyn P. Chipperfield[1,2], Sandip Dhomse[1], Ryan Hossaini[3], Wuhu Feng[1,4], Michelle L. Santee[5], Mark Weber[6], John P. Burrows[6], Jeanette D. Wild[7,8], Diego Loyola[9], Melanie Coldewey-Egbers[9]

1. School of Earth and Environment, University of Leeds, Leeds, UK

[2]National Centre for Earth Observation, University of Leeds, UK.

[3]Lancaster Environment Centre, Lancaster University, Lancaster, UK.

[4]National Centre for Atmospheric Science, University of Leeds, Leeds UK.

[5]Jet Propulsion Laboratory, California Institute of Technology, Pasadena, CA, USA.

[6]Institute of Environmental Physics, University of Bremen, Bremen, Germany.

[7]Innovim LLC, Greenbelt, MD, USA.

[8]NOAA/NCEP/Climate Prediction Center, College Park, MD, USA.

[9]Deutsches Zentrum für Luft- und Raumfahrt (DLR), Institut für Methodik der Fernerkundung (IMF), 82234 Oberpfaffenhofen, Germany.

Contents of this file

Introduction

This document provides Supporting Information for the main GRL paper. This information consists of six supplementary figures and one table which provide further model information or present results for additional latitude bands or for different model runs compared to the main paper.

Text S1.

Table S1 gives the observed mean and ±1σ range of the short-lived chlorine source gases CH_2Cl_2, $CHCl_3$, C_2Cl_4 and $C_2H_4Cl_2$ from aircraft campaigns over the period 2004-2014. The observations were obtained in the tropical upper troposphere (UT, 16.5 – 17.5 km altitude) and so are representative of air which enters the lower stratosphere. The table also gives the sum of chlorine in these 4 species. These 4 species have been included in a TOMCAT simulation with detailed tropospheric chlorine chemistry (Hossaini et al., 2015b). This simulation used ground-based observations for the time-dependent boundary conditions for CH_2Cl_2, $CHCl_3$, and C_2Cl_4. For $C_2H_4Cl_2$ the simulation uses a time-independent but latitude-varying surface mixing ratio based on HIPPO data (Hossaini et al., 2015b). Results from this TOMCAT run with detailed tropospheric chemistry are used here to provide the UT boundary conditions in the stratospheric simulations in this study. These values are given in Table S1 for the same time periods as the campaign. The overall modelled UT VSLS chlorine values are also shown Figure S1 along with the observed campaign values. Overall the table and figure show good agreement between the model and the observations, indicating that the VSLS chlorine trend used in the simulations for the main paper is realistic. We would emphasise that as we find that the chlorine VSLS trend is not a major driver of the observed extratropical ozone variations, our conclusions are not sensitive to moderate uncertainties in this trend.

Figure S2 compares the observed partial or total column ozone from 60°S-60°N with results from TOMCAT simulation CNTL. This is similar to Figure 1 in the main paper but compares the absolute column values. The panels indicate the mean bias between the simulation and the observations (CNTL – observations). Overall the model agrees very well with the observations throughout the stratosphere. Clearly the model simulates the large seasonal cycle well. However, to emphasise the comparisons of the interannual variability the main text presents the comparison in the form of anomalies.

Figure S3 shows comparisons of ozone observed by the Microwave Limb Sounder and the model simulation CNTL for 4 pressure levels between 100 hPa and 10 hPa for the northern hemisphere and southern hemisphere mid-latitude regions. This is similar to Figure 2 in the main paper but compares the absolute mixing ratio values. Again, the plot shows the simulation agrees well with the observations, but in order to focus on the important interannual variability the main text presents the comparisons as anomalies.

Figure S4 shows comparisons of ozone anomalies observed by the Microwave Limb Sounder and the model for 4 pressure levels between 100 hPa and 10 hPa for the tropical regions 20°S-20°N and 35°S-35°N. This complements Figure 2 of the main paper with information on the other latitudes which make up the full 60°S-60°N range (used for example in Figure 1), and a figure which focuses on a usual definition of the tropics.

Figure S5 compares the observed anomalies in partial or total column ozone from 60ºS-60ºN with results from TOMCAT simulations CNTL, NOCl and EXBR. This is similar to Figure 1 in the main paper but with the addition of simulations NOCl and EXBR and only the GTO-ECV dataset in the total column panel. The very close agreement between these runs and the control run CNTL shows again the small effect of the modelled trends in short-lived chlorine and bromine species on column ozone over this time period. Differences between these model simulations are used for the 'Cl-VSLS', and 'Br-VSLS' lines in Figure 4 of the main paper.

Figure S6 compares the observed anomalies in partial or total column ozone from 60ºS-60ºN with results from TOMCAT simulations CNTL, fDYN, fDYN_NOSC, fDYN_NOSC_fAER. This is similar to Figure 1 in the main paper but with the addition of simulations fDYN, fDYN_NOSC, fDYN_NOSC_fAER and only the GTO_ECV dataset in the total column panel. This figure shows the role of different processes in contribution to the observed ozone variations. Differences between these model simulations are used for the 'solar', 'aerosol' and 'dynamics' lines in Figure 4 of the main paper.

Table S1: Observed mixing ratio of chlorine (ppt Cl) from CH_2Cl_2, $CHCl_3$, C_2Cl_4 and $C_2H_4Cl_2$ obtained from high altitude aircraft measurements around the tropical tropopause (16.5-17.5 km). The observed data are mean quantities (± 1σ) obtained from high altitude aircraft during 6 NASA campaigns: Pre-AVE (2004), CR-AVE (2006), TC4 (2007) and ATTREX (2011-2014, e.g. Navarro et al., 2015). The last two columns show observed total chlorine ([2×CH_2Cl_2] + [3×$CHCl_3$] + [4×C_2Cl_4] + [2×$C_2H_4Cl_2$]) and equivalent TOMCAT/SLIMCAT estimates.

Campaign	Year	CH_2Cl_2 (ppt Cl)	$CHCl_3$ (ppt Cl)	C_2Cl_4 (ppt Cl)	$C_2H_4Cl_2$ (ppt Cl)	Total Cl Observed (ppt Cl)	Total Cl Modelled (ppt Cl)
Pre-AVE	2004	23.4 ±1.1	16.4 ±1.3	2.7 ±0.9	3.5 ±0.6	46.1 ±3.9	55.6 ±8.1
CR-AVE	2006	22.9 ±2.2	16.2 ±2.4	1.2 ±0.7	2.5 ±1.3	42.8 ±6.6	58.0 ±8.5
TC4	2007	39.9 ±5.1	16.4 ±2.9	1.3 ±0.6	5.5 ±3.2	63.0 ±11.7	62.5 ±9.3
ATTREX	2011	53.6 ±2.2	13.4 ±0.9	1.4 ±0.8	16.2 ±1.9	84.5 ±5.7	72.0 ±11.6
ATTREX	2013	60.0 ±7.4	18.8 ±1.7	2.2 ±0.7	21.5 ±3.0	102.4 ±12.8	85.9 ±16.1
ATTREX	2014	69.9 ±7.2	19.9 ±1.8	2.0 ±0.5	13.3 ±1.8	105.1±11.3	93.5 ±16.9

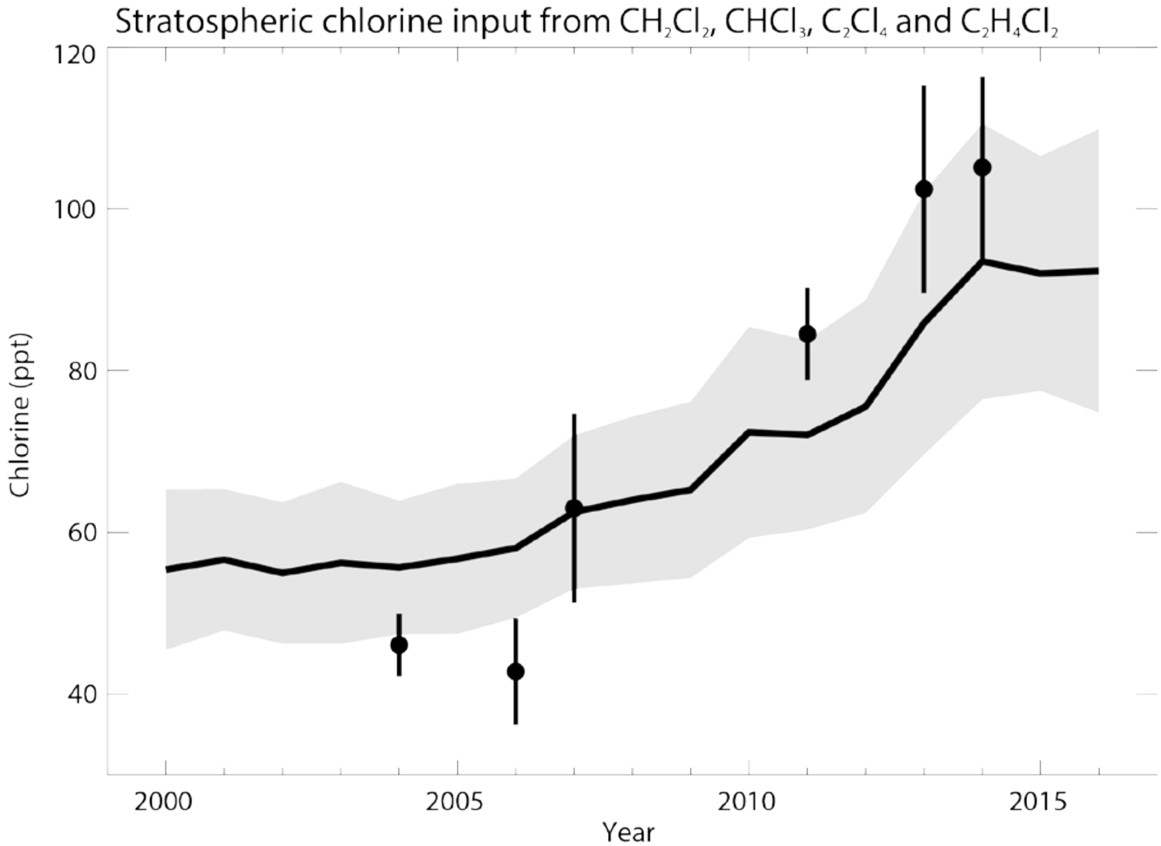

Figure S1. Modelled annual mean total stratospheric chlorine injection (ppt Cl) from CH_2Cl_2, $CHCl_3$, C_2Cl_4 and $C_2H_4Cl_2$ (solid line, shading denotes ± 1σ); update of Hossaini et al. (2015b). Total chlorine injection defined as: [2×CH_2Cl_2] + [3×$CHCl_3$] + [4×C_2Cl_4] + [2×$C_2H_4Cl_2$] at the tropical tropopause. Also shown is the mean chlorine injection from available high-altitude aircraft data (filled circles, vertical bars denote ± 1σ). See Table S1.

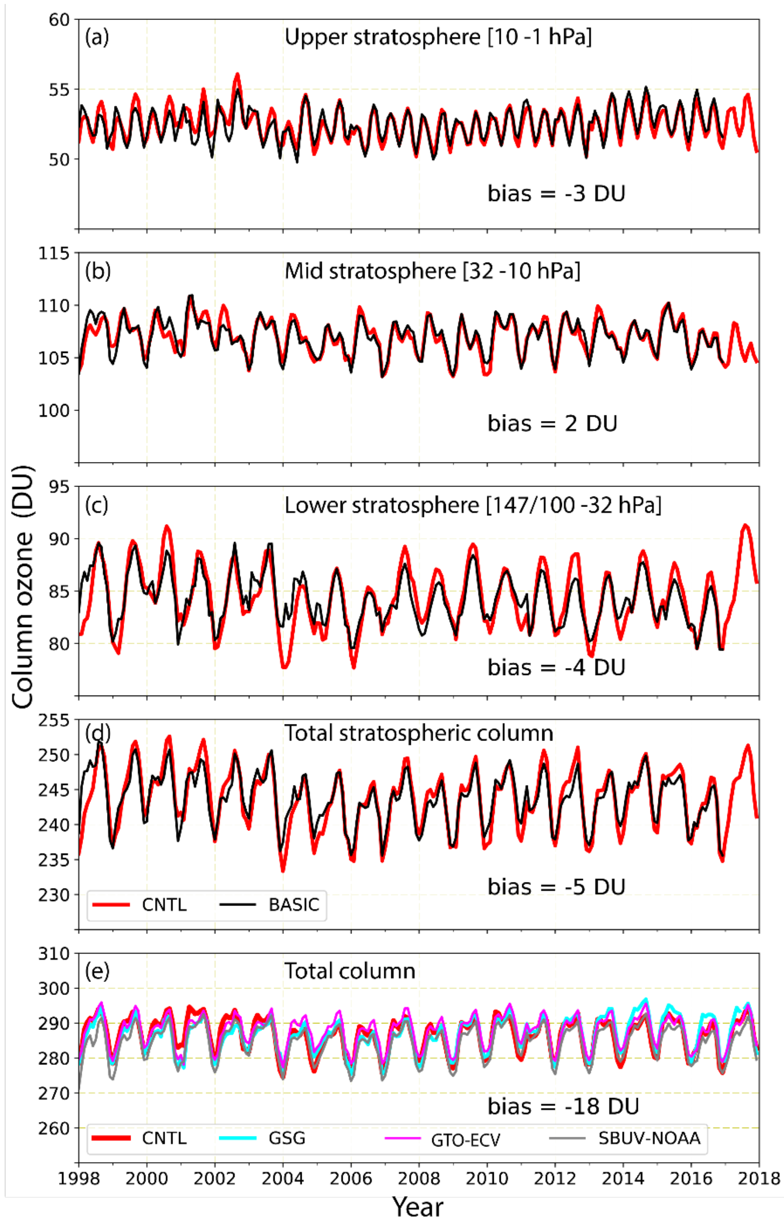

Figure S2. Column ozone (DU) averaged from 60°S – 60°N for (a) upper stratosphere (10-1 hPa), (b) middle stratosphere (32-10 hPa), (c) lower stratosphere (147/100-32 hPa), (d) total stratosphere and (e) total column for 1998-2017 from TOMCAT control simulation CNTL. Panels (a)-(d) also show results from the BASIC dataset (Ball et al., 2018) for 1998-2016. Panel (e) also shows observations from GSG, GTO-ECV and SBUV-NOAA for 1998-2017. Similar to Figure 1 in the main text but for absolute ozone column rather than the anomaly. Each panel indicates the mean bias (DU) for the model minus observations. The bias in panel (e) is calculated relative to the GSG dataset.

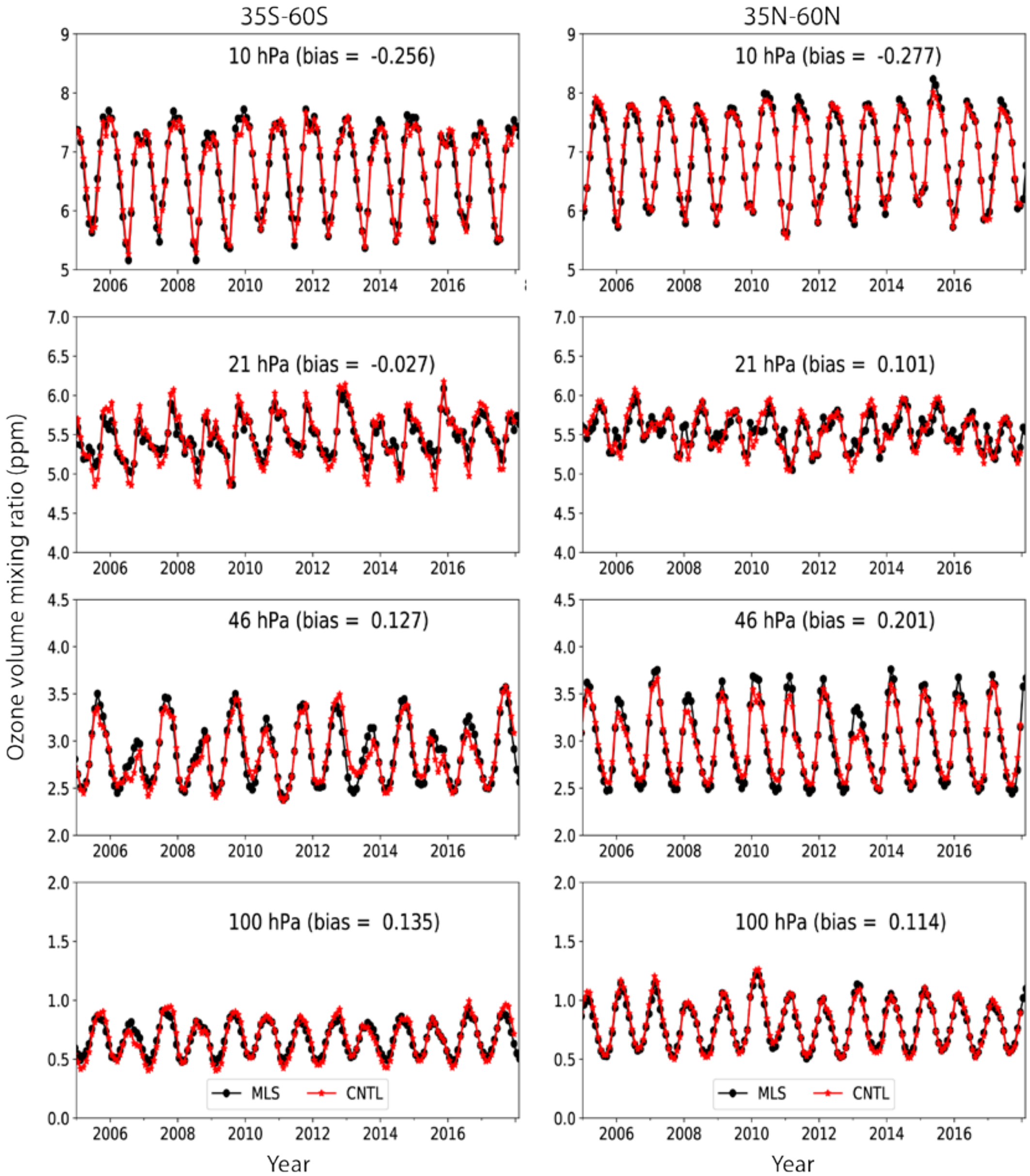

Figure S3. Monthly mean stratospheric ozone (ppm) observed by the Microwave Limb Sounder (MLS, black line) from 2005 to 2017 at 10, 21, 46 and 100 hPa pressure levels for (left) 35°S-60°S and (right) 35°N-60°N. Also shown are results from the TOMCAT control simulation CNTL (red line) for 2004-2017. Similar to Figure 2 in the main text but for absolute ozone volume mixing ratio rather than the anomaly. Each panel indicates the mean bias (ppm) for the model minus observations.

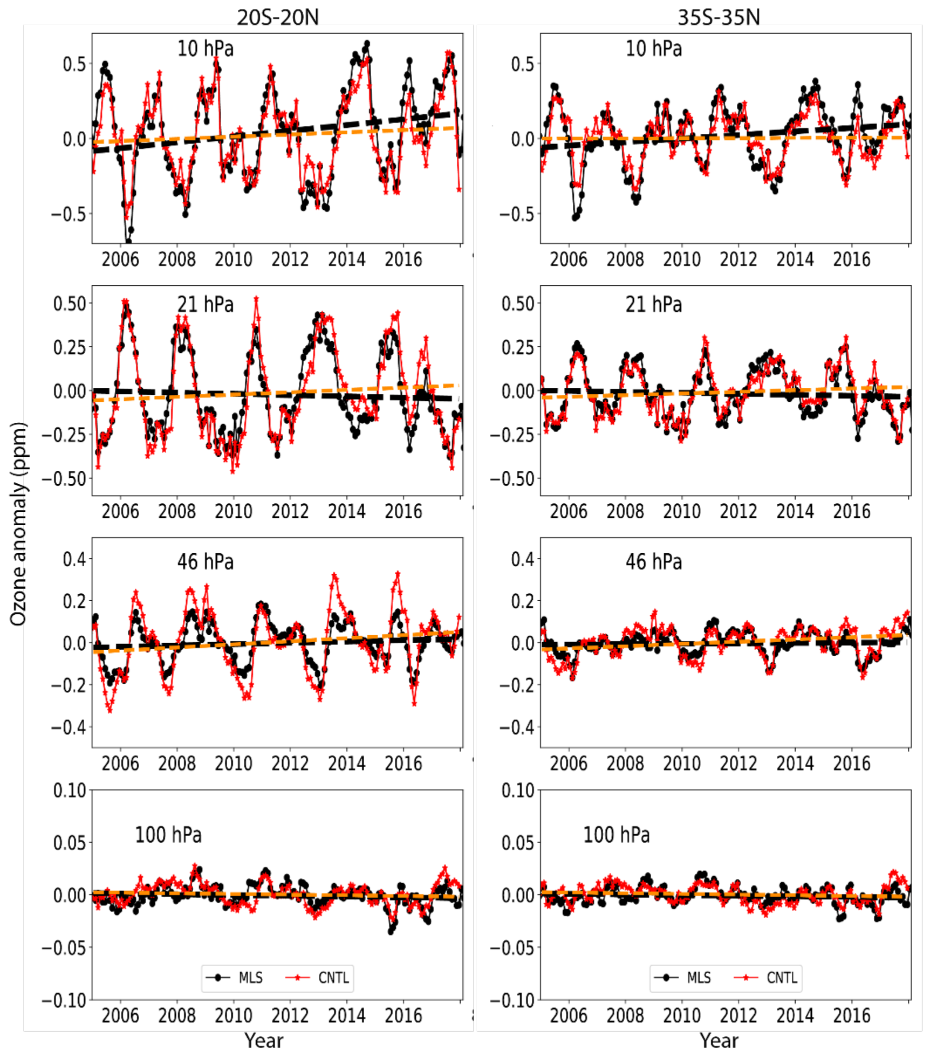

Figure S4. Observed anomaly in monthly mean stratospheric ozone (ppm) at 4 levels for (left) 20°S-20°N and (right) 35°S-35°N derived from Microwave Limb Sounder data for 2005-2017. Also shown are results from the TOMCAT control simulation CNTL for 2005-2017. The anomalies are calculated with respect to the 2005-2017 monthly means.

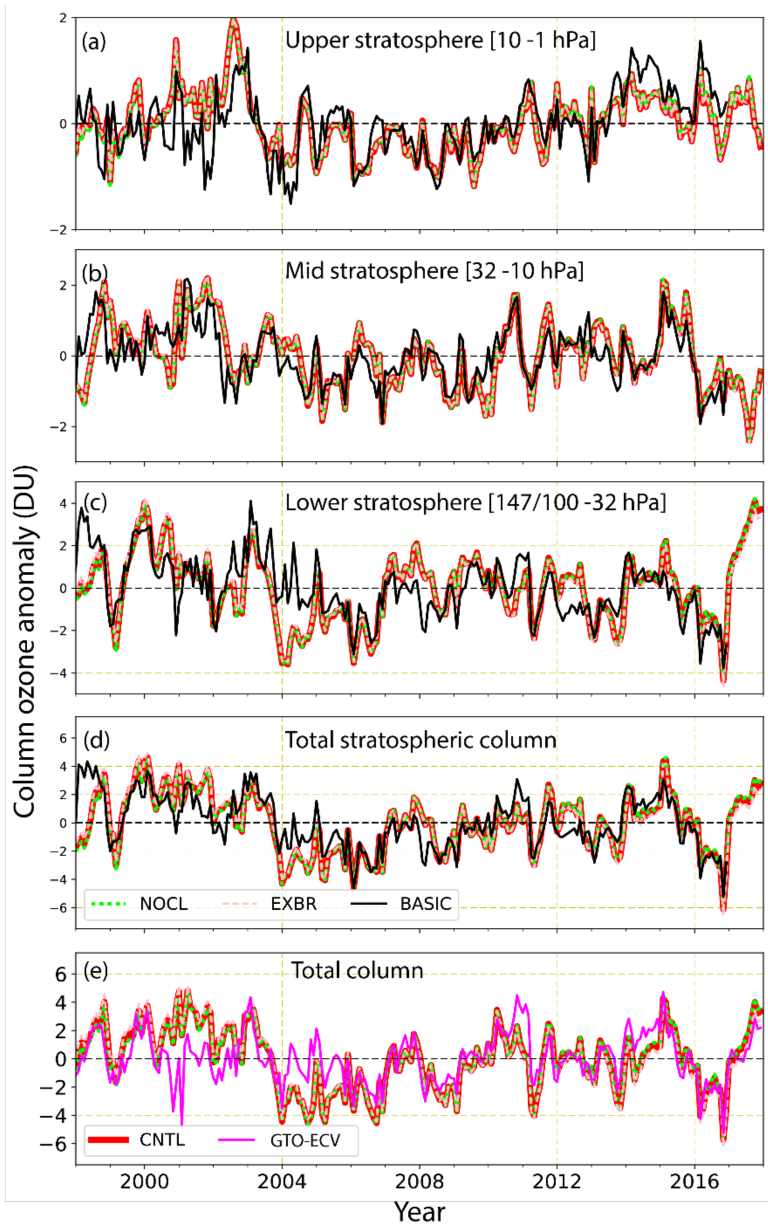

Figure S5. Anomaly in column ozone (DU) averaged from 60°S – 60°N for (a) upper stratosphere (10-1 hPa), (b) middle stratosphere (32-10 hPa), (c) lower stratosphere (147/100-32 hPa), (d) total stratosphere and (e) total column for 1998-2017 from TOMCAT simulations CNTL, NOCL and EXBR. Panels (a)-(d) also show results from the BASIC dataset (Ball et al., 2018) for 1998-2016. Panel (e) also shows observations from GTO-ECV for 1998-2017. The anomalies are calculated with respect to the 1998-2016 monthly means.

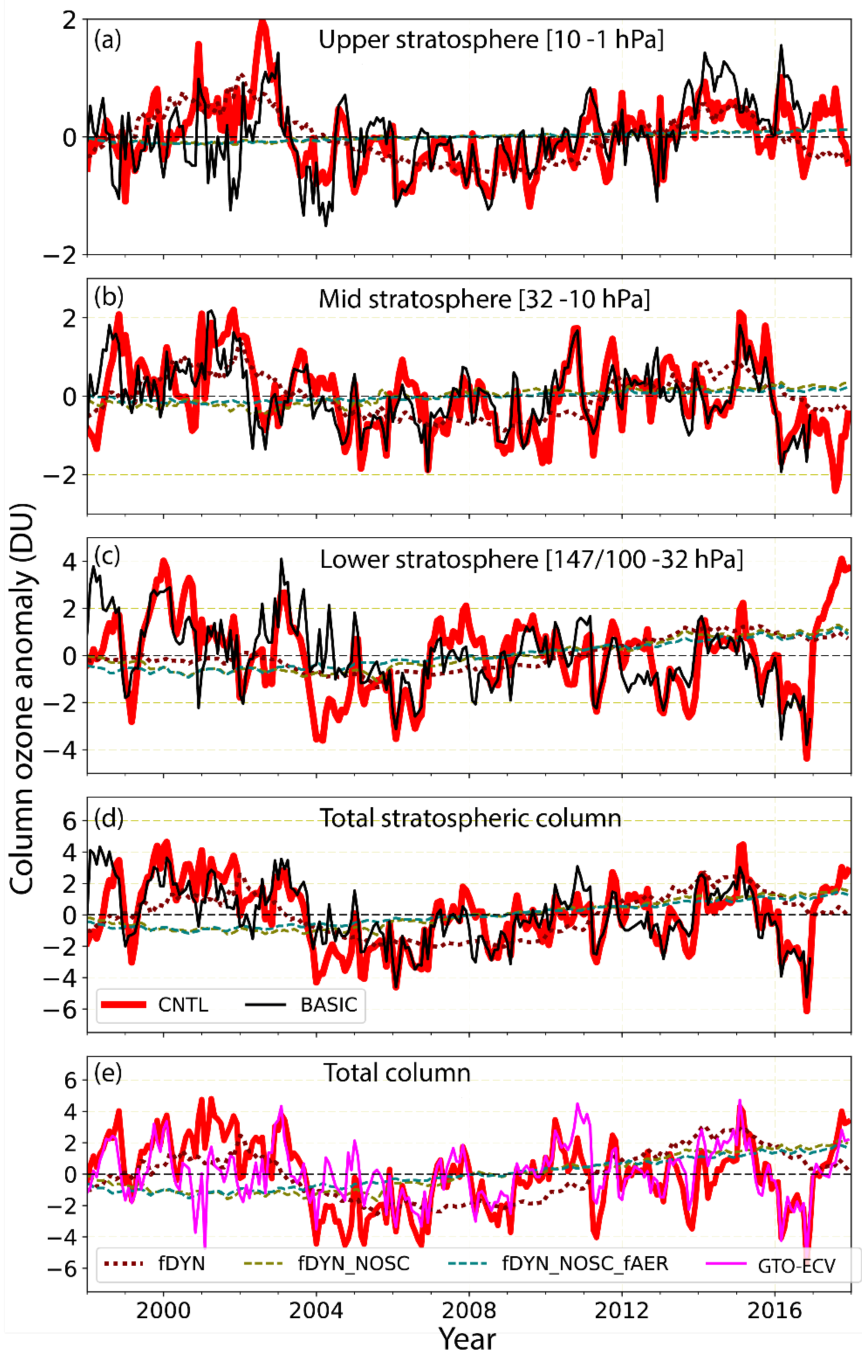

Figure S6. Anomaly in column ozone (DU) averaged from 60°S – 60°N for (a) upper stratosphere (10-1 hPa), (b) middle stratosphere (32-10 hPa), (c) lower stratosphere (147/100-32 hPa), (d) total stratosphere and (e) total column for 1998-2017 from TOMCAT simulations CNTL, fDYN, fDYN_NOSC and fDYN_NOSC_fAER. Panels (a)-(d) also show results from the BASIC dataset (Ball et al., 2018) for 1998-2016. Panel (e) also shows observations from GTO-ECV for 1998-2017. The anomalies are calculated with respect to the 1998-2016 monthly means.